Materials Research Express

PAPER

Investigation on microstructures and mechanical behavior of *in-situ* synthesized TiC and TiB reinforced Ti6Al4V based composite

To cite this article: Bowen Zheng *et al* 2019 *Mater. Res. Express* **6** 116597

Materials Research Express

PAPER

Investigation on microstructures and mechanical behavior of *in-situ* synthesized TiC and TiB reinforced Ti6Al4V based composite

RECEIVED
7 August 2019

REVISED
24 September 2019

ACCEPTED FOR PUBLICATION
1 October 2019

PUBLISHED
18 October 2019

Bowen Zheng[1], **Fuyu Dong**[1,5], **Xiaoguang Yuan**[1,5], **Yue Zhang**[1], **Hongjun Huang**[1], **Xiaojiao Zuo**[1], **Liangshun Luo**[2], **Liang Wang**[2], **Yanqing Su**[2], **Xuan Wang**[3] and **Peter K Liaw**[4]

[1] School of Materials Science and Engineering, Shenyang University of Technology, Shenyang 110870, People's Republic of China
[2] School of Materials Science and Engineering, Harbin Institute of Technology, Harbin 150001, People's Republic of China
[3] School of Materials Science and Engineering, Chongqing University, Chongqing 400044, People's Republic of China
[4] The Department of Materials Science and Engineering, The University of Tennessee, Knoxville, TN, United States of America
[5] Authors to whom any correspondence should be addressed.

E-mail: dongfuyu2002@163.com **and** yuanxg@sut.edu.cn

Keywords: titanium matrix composite, microstructure, compressive strength, wear properties

Abstract

To enhance the friction and wear behavior of the Ti6Al4V alloy, titanium matrix composites (TMCs) were prepared by the single TiC, single TiB, and (TiC + TiB) hybrid reinforced with the volume fraction of 2, 6, and 10%, respectively. To investigate the effect of reinforcements on compressive and wear properties, the x-ray Diffraction (XRD), Scanning Electron Microscope (SEM), Electron Probe Micro-analyzer (EPMA), compression test, and pin-on-disk friction tests were applied. The results indicated that compressive strength increased with the addition of the reinforcement, and wear properties were improved due to the uniform distribution of reinforcements, which enhanced the resistance against tangential forces associated with the sliding wear. The wear mechanism appeared to be mainly based on the severe adhesive and oxidative wear, gradually transitioned to slight adhesion, abrasive, and oxidative wear.

1. Introduction

Titanium alloys are widely applied in the industrial production due to their excellent properties. However, it has some weak points, such as the low surface hardness and poor tribological resistance, limiting wider applications in certain fields [1–3]. In order to expand the application of titanium alloys, several recent studies showed that the creep and wear properties of titanium alloys were improved remarkably by adding hard particles, and higher specific strengths were obtained at room and high temperatures [4–8]. The discontinuous reinforced titanium matrix composites had the characteristics of isotropy, simple preparation process, and low manufacturing cost. The SiC, TiC, TiB, TiB_2, Al_2O_3, and BN were generally considered as reinforced candidates, which could enhance stiffness, strength, and elevated-temperature performance [9–12]. Moreover, the high elastic modulus and excellent strength of TiB and TiC were considered as the optimal choice due to their thermal expansion coefficient and density close to those of the titanium alloy. The different preparation methods played a vital function in deciding the properties of metal matrix composites, which resulted in different binding interfaces between the matrix and reinforcement [13–18]. *In-situ* synthesized TMCs was fabricated by a casting method to ensure the clean interface and no interfacial reactions, thus achieving a good combination of properties in the obtained metal matrix and reinforcements [19, 20]. Although there have been many studies regarding mechanical properties, such as tensile, fatigue, and creep, most studies have only focused on the process technology, including extrusion, forging, and powder metallurgy, they have paid little attention to the friction mechanism and wear properties of particulate-reinforced TMCs during use [21, 22]. Moreover, TMCs exhibits high specific strengths and moduli, excellent fatigue and creep properties, outstanding high-temperature performance and corrosion resistance [23], which are applicable to brake disc materials for automobiles.

Table 1. Properties of the matrix alloy and reinforcements used in TMCs [27].

Materials	Density ($g \cdot cm^{-3}$)	Melting point (K)	linear expansion coefficient (10^{-6} K^{-1})	E-Modulus (GPa)
TC4	4.44	1,933	9.39	110
TiB	4.57	2,473	8.6	550
TiC	4.93	3,433	6.52 ~ 7.15 (25 ~ 500 °C)	440

Compared with the traditional cast iron brake disc, TMCs have a lower density and more excellent corrosion resistance, so they are expected to become a new type of brake disc materials.

In fact, the friction process was considered to be an extremely complex process, not only related to the friction condition, but also to the material structure [24–26]. So far, the acquaintance of wear behavior and mechanisms of titanium matrix composites was quite limited. Therefore, with the rapid development of titanium matrix composites in engineering applications, it was urgent to make an in-depth research on the sliding wear of titanium matrix composites.

In this study, the single TiC, single TiB, and (TiB + TiC) hybrid reinforced Ti6Al4V (TC4) composites were prepared, which were fabricated through *in situ* reactions, including Ti + C → TiC, Ti + TiB_2 → 2TiB, and 5Ti + B_4C → 4TiB + TiC. To better understand the effect of the reinforcement compositions on microstructures, compression performance, and wear properties of TMCs against forged steel, Cr12MoV, the microstructures of different reinforcement compositions, wear surface, and cross-sectional surface were investigated.

2. Experimental procedure

The B_4C powders (98%, ave. particle size, 50 μm), TiB_2 powders (99%, ave. particle size, 50 μm), and C powders (99.8%, ave. particle size, 5–7μm) were added into Ti6Al4V (TC4) alloy with a chemical composition of 6.21% Al, 4.0%V, 0.02%Fe, 0.012%C, 0.13%O, 0.005%N, Bal. Ti weight percent (wt%) to prepare composites with different compositions, respectively. Table 1 shows physical properties of the matrix alloy and reinforcements. It can be seen from the table 1 that the densities of TiC and TiB were 4.93 and 4.57 $g{\cdot}cm^{-3}$, respectively, and their linear expansion coefficients were close to the TC4 alloy. Besides, the melting points and elastic moduli of the two reinforced phases were larger than that of the TC4 matrix alloy. So it was not difficult to imagine that TiC and TiB as reinforced phases of TMCs will be a good choice. The single TiC and TiB reinforced composites were synthesized as the 2, 6, and 10% volume fractions, and those of *in situ* (TiB + TiC) with a 1/1 ratio reinforced titanium matrix composites (TMCs) were also 2, 6, and 10%.

To acquire homogeneous composite structures, the melting-casting process was more than 4 times by the vacuum arc melting furnace and finally cooled in a water-cooled copper crucible. The *in-situ* reactions during the melting process were described as follows:

$$Ti + C \rightarrow TiC \quad (1)$$

$$Ti + TiB_2 \rightarrow 2TiB \quad (2)$$

$$5Ti + B_4C \rightarrow 4TiB + TiC \quad (3)$$

The metallographic observation, composite-phase identification, surface morphology, and elemental distribution of worn surfaces were determined, using a Hitachi S-3400N type scanning electron microscope (SEM; Hitachi High-Technologies Corp., Tokyo, Japan), a Shimadzu XRD-7000 type x-ray diffractometer, and a Shimadzu EPMA-1720 type electron probe micro-analyzer (Shimadzu Corp., Kyoto, Japan). Hardness of composite materials was measured, using an HR-150A-type Rockwell hardness tester with a 1,000 g load for a sustained time of 15 s. The compression test was tested by a WDW-100KN-M electronic universal testing machine at the speed of 2 mm min^{-1}., and the samples with 3 mm in diameter and 6 mm in height were obtained from the ingots. The dry friction and wear experiments were performed using a pin-on-disc friction test apparatus (MMU-5G, Sida Tester Co. Ltd, Jinan, China) with the forged steel of Cr12MoV (58–60HRC) as the grinding material, samples at Φ4 × 15 mm, and applied load set at a 100 N load (corresponding to an initial mean contact stress of 17 MPa) for 30 min with a sliding speed of 0.11 m s^{-1}, in order to ensure the accuracy of the experimental data, the experiments need to be repeated three times in the same condition.

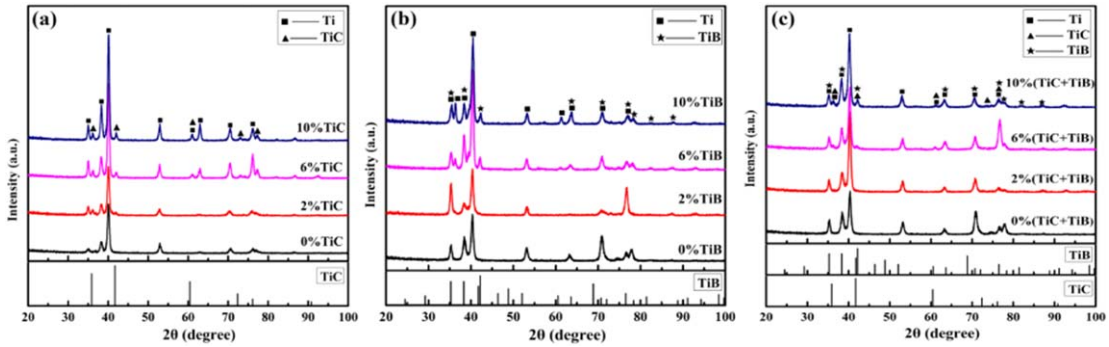

Figure 1. XRD analysis of TMCs with different reinforcement compositions. (a) TiC, (b) TiB, and (c) TiB + TiC.

3. Results and discussion

3.1. Microstructure and composition

Figure 1 shows the XRD analysis of TMCs with different reinforcement compositions. No traces of the residual B_4C, TiB_2, and C were detected by XRD, which indicated that *in-situ* reaction was completed, and Al and V elements could be considered as solid solutions in the matrix. The existence of Ti and TiC phases could be observed (figure 1(a)), which indicated that the reaction as Ti + C → TiC occurred during the melting process. The peak intensity of TiC increased gradually with the increase of the additive content, which exhibited that the content of the TiC-reinforced particle increased. Figure 1(b) shows that the composites were predominantly composed of Ti and TiB phases, which illustrated that the *in-situ* reaction as Ti + TiB_2 → 2TiB was completed, and the variation of the TiB peak intensity coincided with the addition. The presence of Ti, TiB, and TiC peaks could be detected in figure 1(c). This trend displayed that the *in-situ* reaction among Ti, C, and B_4C has happened as follows, Ti + C → TiC, and 5Ti + B_4C → 4TiB + TiC, the volume fractions of *in situ* (TiB + TiC) with a 1/1 ratio reinforced TMCs could be obtained by the above two reactions.

Figure 2 shows SEM images of TMCs with different reinforcement compositions. Figure 3 displays the EDS analysis of TMCs with different regions of (a) 2 vol% TiC, (b) 2 vol% TiB, (c) and (d) 2 vol% (TiC + TiB). Based on the EDS results, the reinforcement phases were determined as TiC (figure 3(a)). When the TiC volume content was 2%, TiC presented two shapes: one was equiaxed or nearly equiaxed, the other was fine granular or short rod, which corresponded to primary TiC and eutectic TiC, respectively. It could be observed that the primary TiC was the majority, and the eutectic TiC content was low. With the increase of the TiC content, the size of the primary TiC increased, and part of the eutectic TiC grew into the dendrite (figure 2(b)). As the TiC content was 10%, the growth of the dendrite was more obvious in figure 2(c). The crystal structure of TiC was B1-type face-centered cubic, the occupancy of Ti and C atoms was centro-symmetric with no preferential growth direction and growth surface, which led to the same growth rate of TiC on the symmetrical crystal plane. Hence, it was easy to form a centrosymmetrical structure, i.e., an equiaxed or approximately equiaxed morphology. The evolution of TiC into the dendritic morphology could be explained by the theory of constitutional supercooling [28]. The higher the C content was, the larger the crystallization temperature range of the primary TiC was, which led to higher constitutional supercooling in front of the interface of the primary TiC. Therefore, it was easier to form a dendrite morphology.

The crystal structure of TiB was an orthorhombic B27 crystal, and the growth rate along the [010] direction was obviously faster than other directions, which was easier to form whiskers or short fibers. By the EDS analysis of the needle-like phase, the results showed that the contents of B and Ti were 51.62% and 46.05%, respectively, and the atomic ratio of Ti/B was close to 1:1. Therefore, it can be identified that the boride formed was TiB (figure 3(b)). It was found that the short and long needle-like TiB whiskers were observed in figure 2(d), the aspect ratio increased with the addition of TiB (figure 2(e)), and the long needle-like TiB whisker occupied the majority of the matrix (figure 2(f)). Moreover, the microstructure of TMCs could be refined by adding the reinforcement phase. On the one hand, it was because of the B element precipitated from the β phase during the solidification process, which led to the B element enrichment in a liquid phase and constitutional supercooling. This trend provided a driving force for the nucleation of the β phase and improved the nucleation rate of the β phase. On the other hand, it was due to the fact that the excessive B element at the solid-liquid interface decreased the growth rate of the β phase grain, which also reduced the size of the original β grain in TMCs.

When the (TiC + TiB) content was 2%, TiC was mostly rod-like or granular, and TiB was short needle-like (figure 2(g)), and their results were identified by the EDS analysis (figures 3(c) and (d)). With the increase of the content, TiC gradually became equiaxed, and TiB grew longer (figure 2(h)). When it increased to 10%, there was

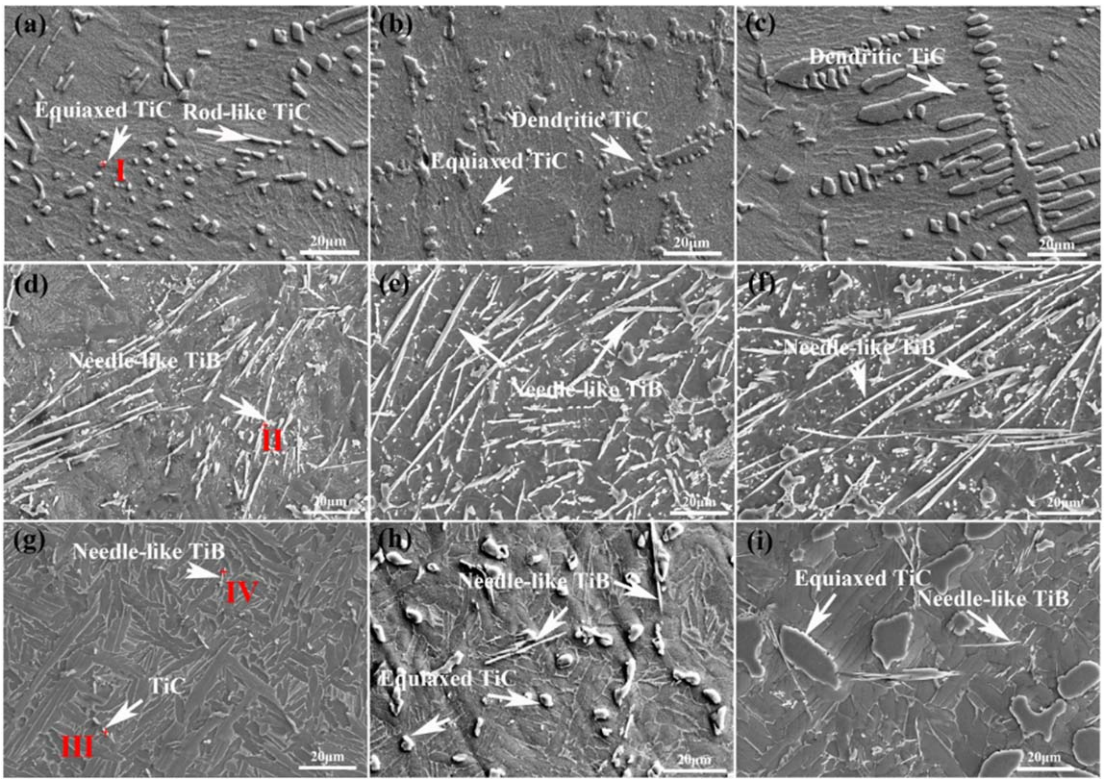

Figure 2. SEM images of TMCs with different reinforcement compositions. (a) 2 vol% TiC, (b) 6 vol% TiC, (c) 10 vol% TiC, (d) 2 vol% TiB, (e) 6 vol% TiB, (f) 10 vol% TiB, (g) 2 vol% (TiC + TiB), (h) 6 vol% (TiC + TiB), (i) 10 vol% (TiC + TiB).

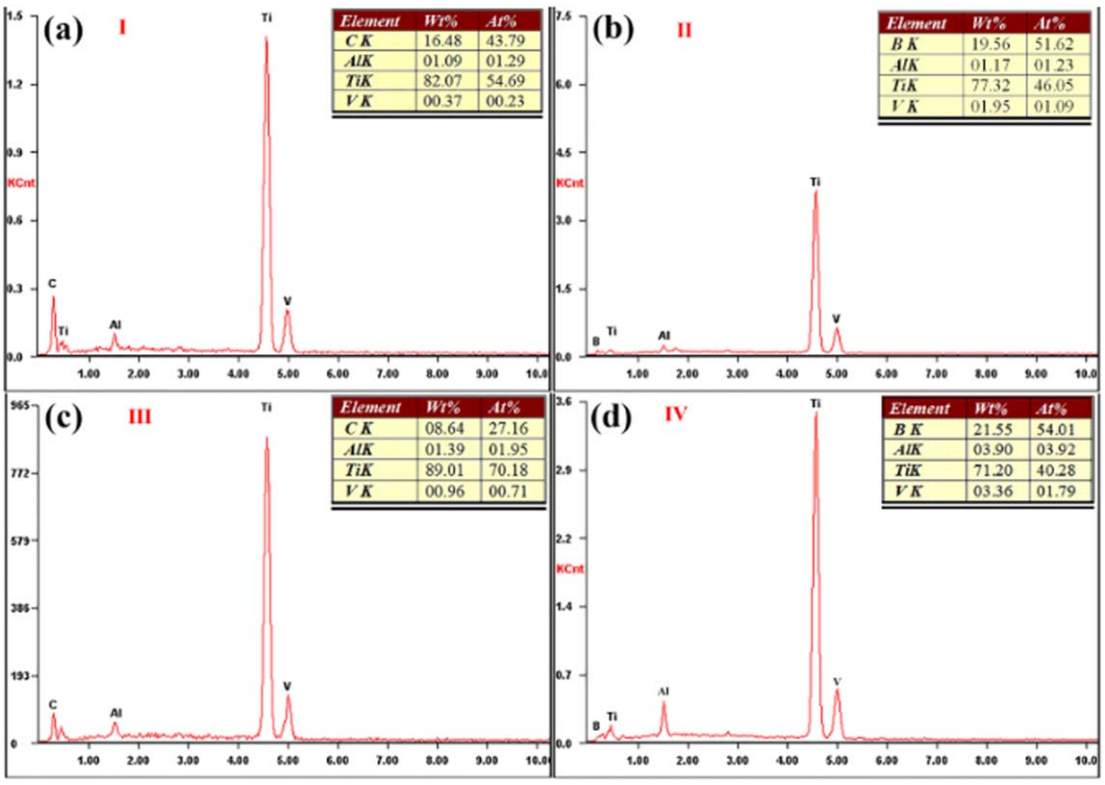

Figure 3. EDS analysis of TMCs with different regions of (a) 2 vol% TiC, (b) 2 vol% TiB, (c) and (d) 2 vol% (TiC + TiB).

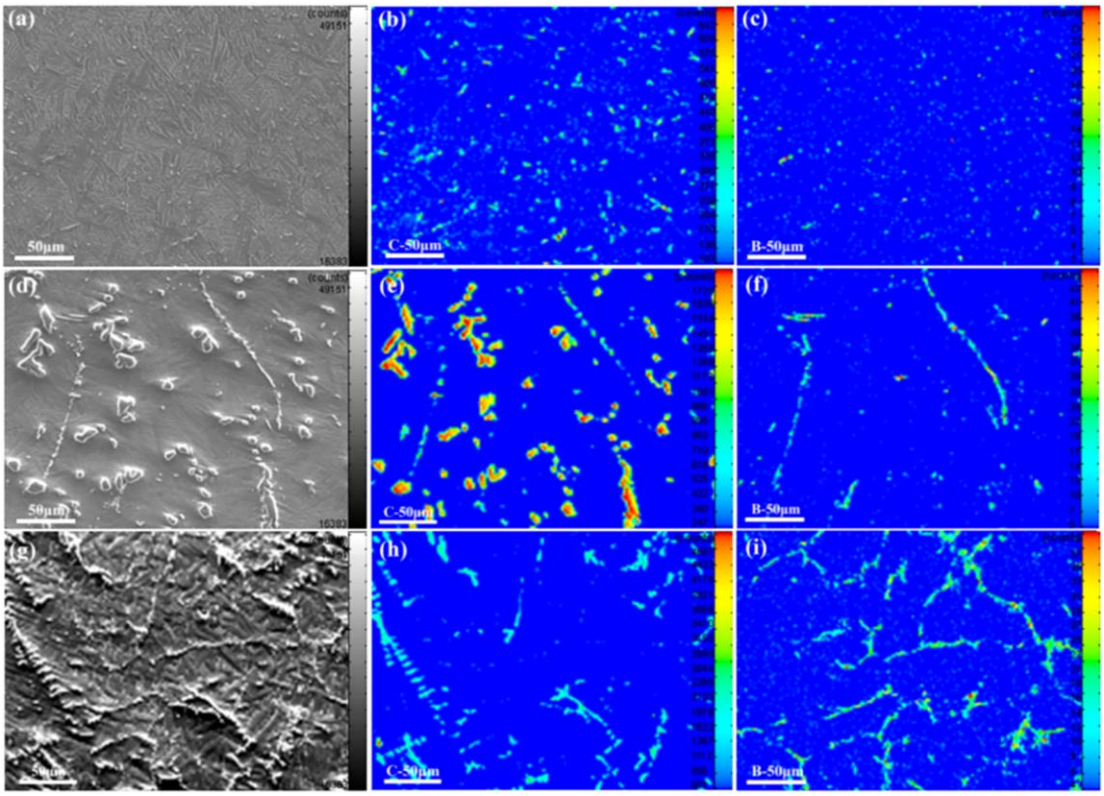

Figure 4. EPMA spectra of TMCs with different reinforcement compositions. (a)–(c) 2% (TiC + TiB), (d)–(f) 6% (TiC + TiB), (g)–(i) 10% (TiC + TiB).

almost no large dendritic TiC. It was mainly due to the formation and growth of TiB along with the TiC, and the formation of TiB hindered the growth of TiC. Furthermore, it was found that the two enhancement phases had a tendency of interdependent and segregated growth. This feature was due to the fact that the first precipitated phase became another heterogeneous nucleation particle, which nucleated near the first precipitated phase, then grew up together, and finally formed TiC and TiB interdependent morphologies.

Figure 4 shows the EPMA elemental maps of (TiC + TiB)/TC4 composites. The results showed that reinforcements were comprised of needle-like TiB and equiaxed TiC particles, which were uniformly distributed in the matrix. The interface between the reinforcement phase and matrix was clean and well bonded without any other impurities. With the increase of the (TiC + TiB) content, the needle-like TiB formed similar reticular structures, which could significantly enhance the strength of composites. The confirmation of the reinforcing structure compositions also validated that the reactions $5Ti + B_4C \rightarrow 4TiB + TiC$ and $Ti + C \rightarrow TiC$ had occurred during the *in situ* reaction of Ti, B_4C, and C powders. Furthermore, the reinforcing phase formed by the *in-situ* method had better bonding than that by the external method and was not easy to crack around the reinforced phases.

3.2. Hardness analysis

Figure 5 shows the hardness curves of composites with different reinforcement compositions. The hardness values increased with the increase of the reinforcement content due to the existence of hard TiC and TiB phases. Under the same amount of the phase addition, (TiC + TiB)/TC4 had the highest hardness value based on synergistic effects of the solution strengthening and fine grain strengthening due to dissolving of C and B elements. According to the analysis of figure 2, it could be concluded that the formation of the high-hardness and high-strength particle reinforcement had a good effect on improving the hardness of composites.

3.3. Compressive properties

Figure 6 shows compressive strength curves of TMCs with different reinforcement compositions. Compared with the TC4 alloy, the compressive strength of TiC reinforced composites increased by 130.8 MPa, 624.37 MPa and 389.6 MPa, respectively (figure 6(a)). This trend was due to the synergistic effect of the bearing capacity of TiC, solid-solution strengthening of C, and refinement of the matrix structure. However, the compression rate decreased gradually with the increase of the reinforcement content. It was noteworthy that the 6 vol%TiC/TC4

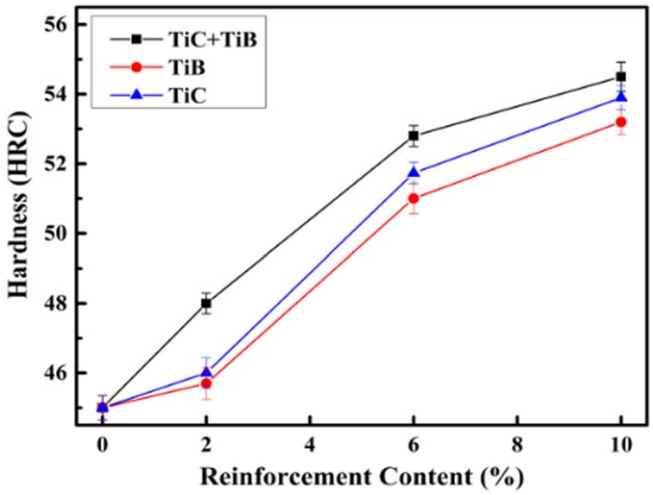

Figure 5. Hardness curves of of TMCs with different reinforcement compositions.

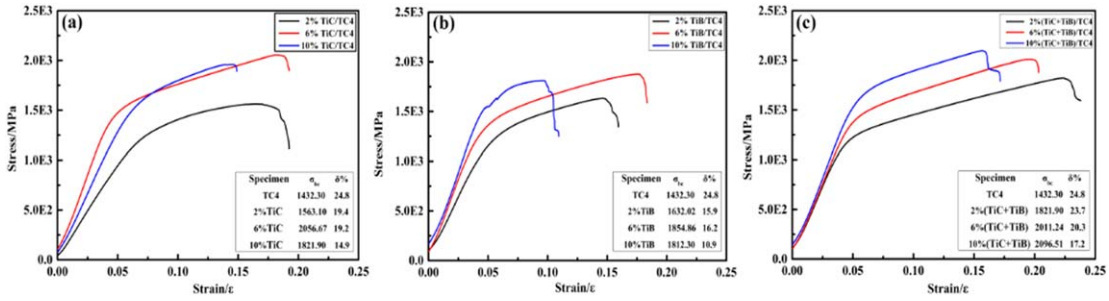

Figure 6. Compressive strength curves of TMCs with different reinforcement compositions. (a) TiC, (b) TiB, and (c) TiB + TiC.

composite has a higher strength than the 10 vol%TiC/TC4 composite, which indicated that the excessive TiC was not conducive to the improvement of room-temperature properties. The strength of TiB reinforced composites rose by 199.72 MPa, 422.56 MPa and 380 MPa, respectively (figure 6(b)), and the compression rate also presented a downward trend. The enhanced effect of (TiB + TiC)/TC4 composites were more pronounced than the single TiC or TiB reinforced composites, and exhibited better plasticity than others. The compressive strength of the composites increased with the rise of the reinforcement content, but the plasticity of the composites decreased considerably with the addition of excessive reinforcements. The strength improvement of composites was mainly attributed to the three factors as described below: the effective bearing capacity of the reinforcement phase; the refinement of the matrix structure; and the effect of solid-solution strengthening. When the composite was subjected to an external load, on one hand, the load transited from the matrix to the reinforcement phases, and the reinforcement phase bore the main load. On the other hand, the existence of the reinforcement phase hindered the dislocation accumulation and movement, which led to the material strengthening. Furthermore, the compression rate of composites was obviously lower than that of the matrix alloy due to both TiC and TiB possessing the high hardnesses and elastic moduli. Deformation began with the relative soft matrix alloys, while the deformation of TiC and TiB lagged behind, which led to the asynchronous deformation between the reinforcements and matrix during the compression process, reducing the plasticity of the composites. Moreover, the stress concentration at the edges of reinforcements could decrease the plasticity of composites, and the bearing capacity of the dendritic TiC was low, which was easier to break under load. Therefore, it was necessary to control the morphology of the reinforcement phase.

3.4. Friction and wear properties

Figure 7 shows the specific wear rate of TMCs with different reinforcement compositions. With the additions of TiC and TiB, the specific wear rate of TMCs was lower than that of TC4 and decreased with the rise of the reinforcement content, which indicated that the wear resistance was effectively improved by adding

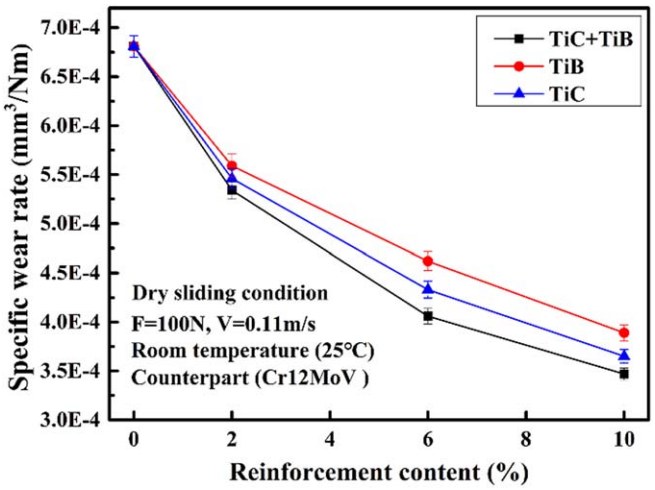

Figure 7. The specific wear rate of TMCs with different reinforcement compositions.

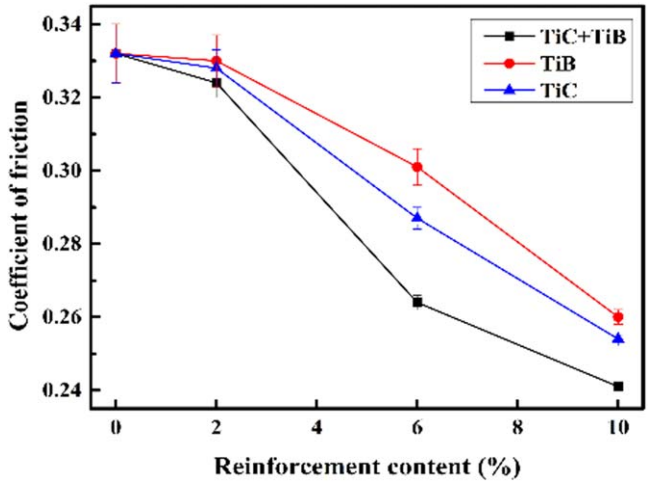

Figure 8. Coefficient of friction of TMCs with different reinforcement compositions.

reinforcements. Moreover, the specific wear rate of the (TiB + TiC) hybrid reinforced composite was lower than that of the single TiC or TiB reinforced material.

Figure 8 presents that the coefficient of friction of the composites was significantly smaller than that of the TC4. On one hand, the strength and hardness of the composites were greatly improved with the addition of different reinforcements. On the other hand, a certain degree of heat was always produced on the wear surface during the friction and wear process, and could not be immediately emitted into the air, which caused the temperature of friction pair rising. For the TC4 alloy, the high coefficient of friction was due to the softening phenomenon with the rise of temperature, which led to the increase of the friction area and coefficient. For composites, the additions of TiB and TiC improved the high-temperature strength and hardness of the composites, controlled effectively the softening degree of the composites caused by the friction heat, and prevented the occlusion phenomenon of the friction pairs, thus decreased the damage of the wear surface and reduced the composite coefficient. Compared to single TiB or TiC reinforced, (TiB + TiC) hybrid-reinforced composite possessed the low friction coefficient corresponding to the variation of the specific wear rate.

Figure 9 shows the wear surface of TMCs with different reinforcement compositions. The plastic deformation, furrows, and adhesive marks of the wear surface were detected by the extrusion and scratch of the friction pins, which exhibited typical characteristics of the adhesive and abrasive wear (figure 9(a)). With the increase of TiC, the adhesive trace of the wear surface decreased, which illustrated that the degree of the adhesive wear reduced, and the abrasive resistance was improved (figure 9(c)). Due to the surface wear during sliding friction, the reinforcement particles were prominent from the matrix, which prevented the direct contact between the matrix and the friction disc. Moreover, the hard reinforcement acted as a load-bearing role due to its

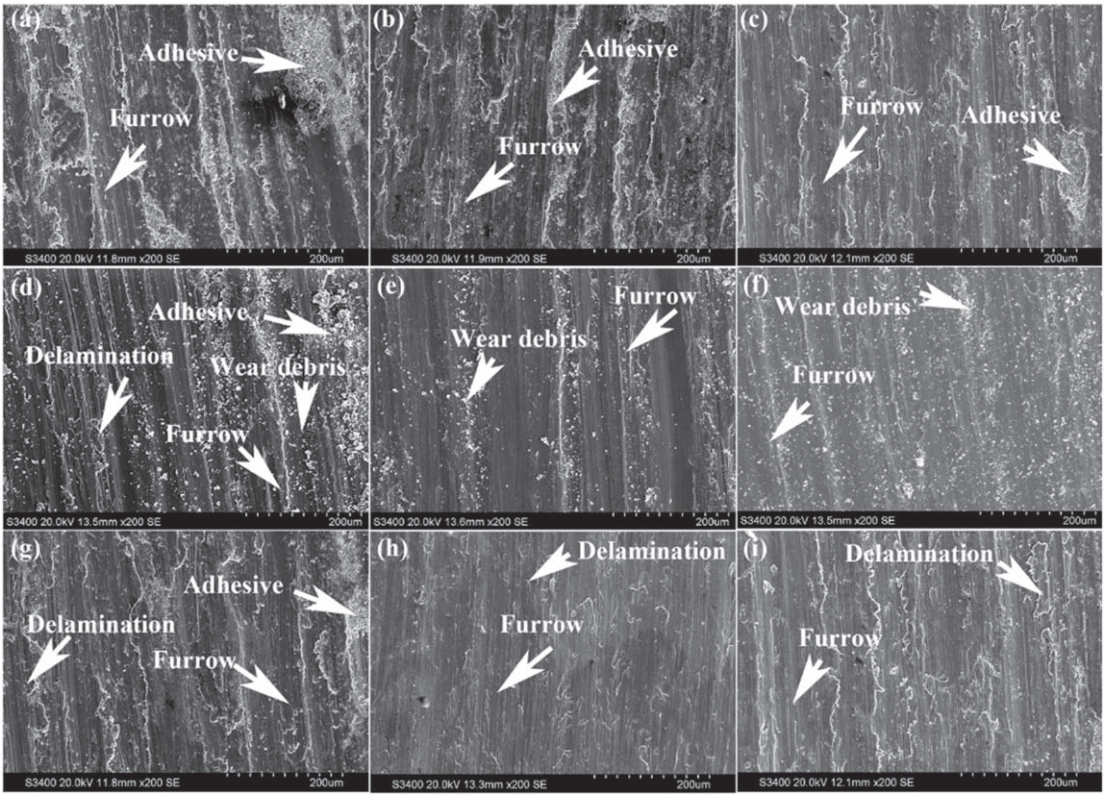

Figure 9. Wear surface of TMCs with different reinforcement compositions. 2 vol% TiC, (b) 6 vol% TiC, (c) 10 vol% TiC, (d) 2 vol% TiB, (e) 6 vol% TiB, (f) 10 vol% TiB, (g) 2 vol% (TiC + TiB), (h) 6 vol% (TiC + TiB), (i) 10 vol% (TiC + TiB).

higher strength and modulus than the matrix alloy. As the content of TiB increased, the amount of adhesive marks and furrows was declined. Thus the main wear mechanism changed from the adhesion to slight and abrasive wear (figures 9(d)–(f)). It can be found that the (TiC + TiB) reinforced composites exhibited the excellent wear resistance, and only slight furrows and delaminations existed on the wear surface (figures 9(g)–(i)). The main wear mechanisms were the slight adhesive and abrasive wear. Moreover, it was noteworthy that the wear surface of the 6 vol% (TiC + TiB) was slightly better than that of the 10vol% (TiC + TiB). This feature was because the wear resistance was not only related to the content, but also the size of the reinforcement. When the content of reinforcements exceeded 6%, the size of the former was relatively smaller than that of the latter (figures 2(h) and (i)), and it was not easy to fall off from the matrix under the action of the force. Thus the fine and uniformlydistributed reinforcement phases could play a more protective role in the matrix alloy.

Figure 10 shows the EPMA analysis of wear cross-section of (TiB + TiC) reinforced composites. It could be found that the Fe element adhered to wear surface of composite due to severe adhesive wear caused by the friction heat (figures 10(a)–(d)). For 6 vol% (TiC + TiB), it could be seen clearly that some C and B elements existed on the surface, and the content of the Fe element was decreased. It indicated the degree of the adhesive wear decreased with the increase of the reinforcement content (figures 10(e)–(h)), and the enhanced effect was more obvious in (figures 10(i)–(l)). The reasons for the improvement of the wear resistance is described as follows: on one hand, the TiC and TiB reinforcements had high strength, hardness, and good wear resistance, which acted as the anti-friction and wear-resistance role. On the other hand, the cross-section of surface indicated that the homogeneous distribution of reinforcement phases in the matrix played a role in dispersion strengthening to enhance the resistance against the tangential stress caused by the sliding wear. This effect was sufficient to enhance the sub-surface strength and ductility of the materials, thus preventing the initiation of micro-cracks during the sliding-wear process.

Figure 11 shows the XRD analysis of the wear surfaces of TMCs with different reinforcement compositions. It was found that the wear surfaces contained matrix Ti, reinforcements, and oxides of TiO_2, FeO and Fe_2O_3. The appearance of Fe element came from the friction disc, which indicated that some Fe element was transferred to wear surface of composite during the wear process. Moreover, as the wear surface temperature rising, the Ti and Fe elements on the surface were easily oxidized leading to the formation of oxides. It can also be observed the worn surface of 6 vol% (TiC + TiB) reinforced TMCs was covered with a dense and continuous tribo-layer analysed on the basis of EPMA, XRD results, which prevented the direct mutual action of contact surfaces and

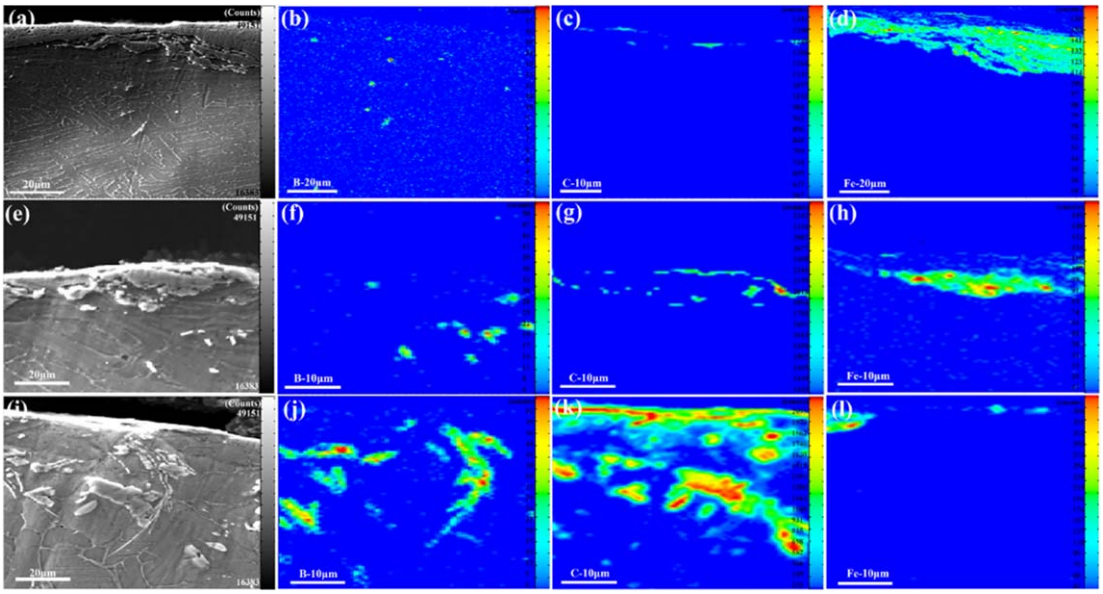

Figure 10. EPMA elemental mapping images of wear cross-section of (TiB + TiC) reinforced composites. (a)–(d) 2 vol% (TiC + TiB), (e)–(h) 6 vol% (TiC + TiB), (i)–(l) 10 vol% (TiC + TiB).

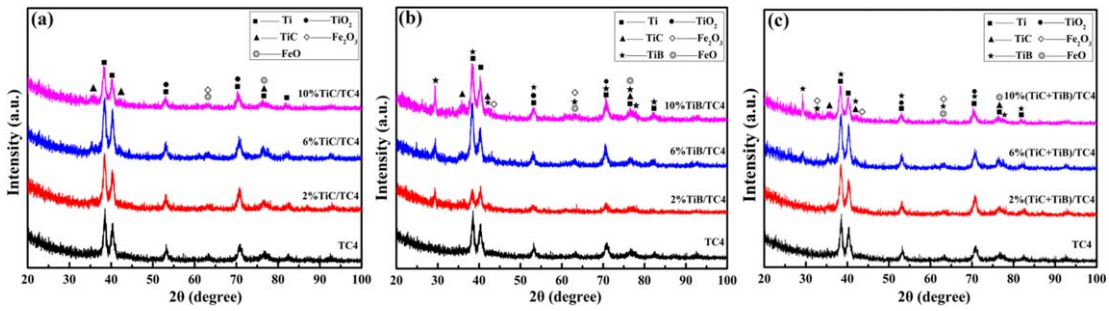

Figure 11. XRD analysis of wear surface of TMCs with different reinforcement compositions. TiC, (b) TiB, (c) TiB + TiC.

formed three body abrasive wear, thus the wear resistance of TMCs was improved. With the increase of the reinforcement content, the peak value of the oxide decreased, which indicated that the adhesive wear and oxidation wear were weakened.

4. Conclusions

(1) For single TiC and TiB reinforced composites, with the increase of the reinforcement content, the morphology of the TiC phase changed from granular to nearly equiaxed shapes, and finally to the dendrite, the shape of TiB grew from short needle-like to long needle-like shapes. For (TiC + TiB) hybrid reinforced composites, the existence of TiB prevented the growth of TiC and made TiC particles smaller with the increase of the TiB content. The addition of reinforcements could refine the matrix to a certain extent.

(2) Compared with the matrix alloy, the compressive strength increased significantly with the increase of the reinforcement content. However, the excessive reinforcement might be not conducive to improving room-temperature performance. In contrast to single TiC and TiB reinforced composites, (TiC + TiB) hybrid reinforced composites possessed better compressive strength and plasticity. That was mainly attributed to the synergistic effect of the bearing capacity of the reinforcement phase, the refinement of matrix structure, and solid-solution strengthening of C.

(3) With the increase of the reinforcement volume fraction, the hardness exhibited an upward trend, and the specific wear rate and coefficient of friction decreased. Owing to the existence of hard reinforcements, the wear resistance had been greatly improved, especially the effect of the (TiC + TiB) hybrid was more

obvious. Furthermore, the reinforcements enhanced the sub-surface strengths and ductilities of the materials, thus preventing the initiation of micro-cracks during the sliding wear process, and a dense and continuous tribo-layer limited the direct interaction of contact surfaces, thus improving the wear resistance of the TMCs. The wear mechanism was transformed from the severe adhesive wear, abrasive wear, and oxidation wear to slight adhesive, abrasive wear, and oxidation wear with the increase of the reinforcement volume fraction.

Acknowledgments

The present work was supported the National Key Research and Development Program of China (2016YFB0301201), and Major Science and Technology Special Plan of Yunnan (2018ZE013), Natural Science Foundation key plan of Liaoning (20180510056), Liaoning Provincial Natural Science Foundation of China (2019-ZD-0216), National Natural Science Foundation of China (51401129, 51871075, and 51875365), Project funded by the China Postdoctoral Science Foundation (2019M653337). PKL thanks the support from the National Science Foundation (DMR-1611180 and 1809640) with the program directors, Drs G. Shiflet and D. Farkas.

ORCID iDs

Bowen Zheng https://orcid.org/0000-0002-4220-5325

References

[1] Li M G, Xiao S L, Xiao L, Xu L J, Tian J and Chen Y Y 2017 Effects of carbon and boron addition on microstructure and mechanical properties of TiAl alloys *J. Alloys Compd.* **728** 206–21
[2] Liu X, Yu D H, Fan Q B and Shi R 2017 Influence of hot rolling and heat treatment on the microstructural evolution of β20C titanium alloy *Materials.* **10** 1071
[3] Zheng B W *et al* 2018 Microstructure, mechanical properties and deformation behavior of new V-free low-cost Ti-6Al-xFe-yCr alloys *Mater. Res. Express* **6** 026551
[4] Banoth R, Sarkar R, Bhattacharjee A, Nandy T K and Nageswara Rao G V S 2015 Effect of boron and carbon addition on microstructure and mechanical properties of metastable beta titanium alloys *Mater. Des.* **67** 50–63
[5] Lin X J *et al* 2019 Hot-deformation behaviour and hot-processing map of melt-hydrogenated Ti6Al4V/(TiB + TiC) *Int. J. Hydrogen Energy* **44** 8641–9
[6] Wang P P, Wang L Q, Lu W J, Qin J N, Chen Y F, Zhang Z W and Zhang D 2010 The effect of heat treatment on mechanical properties of *in situ* synthesized 7715D titanium matrix composites *Materials Science & Engineering:* A **527** 4312–9
[7] Rahoma H K S, Chen Y Y, Wang X P and Xiao S L 2015 Influence of (TiC + TiB) on the microstructure and tensile properties of Ti-B20 matrix alloy *J. Alloys Compd.* **627** 415–22
[8] Imayev V M, Gaisin R A and Imayev R M 2015 Effect of boron additions and processing on microstructure and mechanical properties of a titanium alloy Ti-6.5Al-3.3Mo-0.3Si *Materials Science & Engineering* A **641** 71–83
[9] Huang L J, Geng L and Peng H X 2010 *In situ* (TiB_w+TiC_p)/Ti6Al4V composites with a network reinforcement distribution *Materials Science & Engineering* A **527** 6723–7
[10] Kim J S, Lee K M, Cho D H and Lee Y Z 2013 Fretting wear characteristics of titanium matrix composites reinforced by titanium boride and titanium carbide particulates *Wear* **301** 562–8
[11] Li J X, Wang L Q, Qin J N, Chen Y F, Lu W J and Zhang D 2012 Effect of microstructure on high temperature properties of *in situ* synthesized (TiB + La_2O_3)/Ti composite *Mater. Charact.* **66** 93–8
[12] Kim Y, Yadav P, Hahn J, Xiao X and Lee D B 2019 Oxidation of titanium matrix composites reinforced with (TiB + TiC) particulates *Met. Mater. Int.* **25** 627–32
[13] Attar H, Ehtemam-Haghighi S, Kent D and Dargusch M S 2018 Recent developments and opportunities in additive manufacturing of titanium-based matrix composites: a review *Int. J. Mach. Tools Manuf* **133** 85–102
[14] Ma F C, Wang C H, Liu P, Li W, Liu X K, Chen X H, Zhang K and Han Q Y 2018 Microstructure and mechanical properties of Ti matrix composite reinforced with 5 vol% TiC after various thermo-mechanical treatments *J. Alloys Compd.* **758** 78–84
[15] Wang D J, Zhang R and Yuan S J 2018 Flow behavior and microstructure evolution of a TiB_w/TA15 composite with network-distributed reinforcements during interrupted hot compression *Materials Science and Engineering:* A **725** 428–36
[16] Bai H Q, Zhong L S, Shang Z, Xu Y H, Wu H, Bai J M and Ding Y C 2019 Microstructure and mechanical properties of TiC-Fe surface gradient coating on a pure titanium substrate prepared *in situ J. Alloys Compd.* **771** 406–17
[17] Ballat-Durand D, Bouvier S, Risbet M and Pantleon W 2019 Through analysis of the microstructure changes during linear friction welding of the near-α titanium alloy Ti-6Al-2Sn-4Zr-2Mo (Ti6242) towards microstructure optimization *Mater. Charact.* **151** 38–52
[18] Fu Y Q, Zhou F, Wang Q Z, Zhang M D, Zhou Z F and Li L K Y 2019 The influence of Mo target current on the microstructure, mechanical and tribological properties of CrMoSiCN coatings in artificial seawater *J. Alloys Compd.* **791** 800–13
[19] Gåård A, Hallbäck N, Krakhmalev P and Bergström J 2010 Temperature effects on adhesive wear in dry sliding contacts *Wear* **268** 968–75
[20] Lee J J, Lee J A, Kwon S and Kim J J 2018 Effect of different reinforcement materials on the formation of secondary plateaus and friction properties in friction materials for automobiles *Tribol. Int.* **120** 70–9
[21] Wang L, Zhang Q Y, Li X X, Cui X H and Wang S Q 2014 Severe-to-mild wear transition of titanium alloys as a function of temperature *Tribol. Lett.* **53** 511–20

[22] Li X X, Zhou Y, Ji X L, Li Y X and Wang S Q 2015 Effects of sliding velocity on tribo-oxides and wear behavior of Ti-6Al-4V alloy *Tribol. Int.* **91** 228–34
[23] Patil A S, Hiwarkar V D, Verma P K and Khatirkar R K 2019 Effect of TiB_2 addition on the microstructure and wear resistance of Ti-6Al-4V alloy fabricated through direct metal laser sintering (DMLS) *J. Alloys Compd.* **777** 165–73
[24] Haftlang F, Hanzaki A Z, Abedi H R and Preisler D 2019 The subsurface frictional hardening: a new approach to improve the high-speed wear performance of Ti-29Nb-14Ta-4.5Zr alloy against Ti-6Al-4V extra-low interstitial *Wear* **422–423** 137–50
[25] Verma P C, Ciudin R, Bonfanti A, Aswath P, Straffelini G and Gialanella S 2016 Role of the friction layer in the high-temperature pin-on-disc study of a brake material *Wear. 346-* **347** 56–65
[26] Wang L, Li X X, Zhou Y, Zhang Q Y, Chen K M and Wang S Q 2015 Relations of counterface materials with stability of tribo-oxide layer and wear behavior of Ti-6.5Al-3.5Mo-1.5Zr-0.3Si alloy *Tribol. Int.* **91** 246–57
[27] Grützner S, Krüger L, Radajewski M and Schneider I 2018 Characterization of *in-situ* TiB/TiC particle-reinforced Ti-5Al-5Mo-5V-3Cr matrix composites synthesized by solid-state reaction with B_4C and graphite through SPS *Metals* **8** 377
[28] Wang H W, Qi J Q, Zou C M and Wei Z J 2012 Effect of microstructural characteristics on room temperature tensile properties of *in situ* synthesised TiC/TA15 composite *Mater. Sci. Technol.* **28** 597–602